Journal of Cell Science 111, 1613-1622 (1998)
Printed in Great Britain © The Company of Biologists Limited 1998
JCS7254

Patterns of free calcium in zebrafish embryos

Robbert Créton[1], Johanna E. Speksnijder[2] and Lionel F. Jaffe[1]

[1]Marine Biological Laboratory, Woods Hole, MA 02543, USA
[2]Department of Genetics, Biological Center, University of Groningen, 9751 NN Haren, The Netherlands
*Author for correspondence (e-mail: rcreton@mbl.edu)

Accepted 3 April; published on WWW 27 May 1998

SUMMARY

Direct knowledge of Ca^{2+} patterns in vertebrate development is largely restricted to early stages, in which they control fertilization, ooplasmic segregation and cleavage. To explore new roles of Ca^{2+} in vertebrate development, we injected the Ca^{2+} indicator aequorin into zebrafish eggs and imaged Ca^{2+} throughout the first day of development. During early cleavages, a high Ca^{2+} zone is seen in the cleavage furrows. The high Ca^{2+} zone during first cleavage spreads as a slow wave (0.5 μm/second) and is preceded by three Ca^{2+} pulses within the animal pole region of the egg. When Ca^{2+} concentrations are clamped at the resting level by BAPTA buffer injection into the zygote, all signs of development are blocked. In later development, Ca^{2+} patterns are associated with cell movements during gastrulation, with neural induction, with brain regionalization, with formation of the somites and neural keel, with otic placode formation, with muscle movements and with formation of the heart. Particularly remarkable is a sharp boundary between high Ca^{2+} in the presumptive forebrain and midbrain versus low Ca^{2+} in the presumptive hindbrain starting at 10 hours of development. When Ca^{2+} changes are damped by injection of low concentrations of BAPTA, fish form with greatly reduced eyes and hearts. The present study provides a first overview of Ca^{2+} patterns during prolonged periods of vertebrate development and points to new roles of Ca^{2+} in cellular differentiation and pattern formation.

Key words: Calcium signaling, Imaging, Aequorin, Cell cycle, Differentiation, Pattern formation, Central nervous system, *Danio rerio*

INTRODUCTION

The intracellular concentration of free Ca^{2+} is generally low, in the order of 0.1 μM, but can rapidly increase to reach values in the 1 μM or even 10 μM range. When elevated, Ca^{2+} activates a wide variety of intracellular events such as contraction, secretion, and gene expression (Ghosh and Greenberg, 1995; Ginty, 1997). With this broad range of effects, Ca^{2+} should be an important regulator in embryonic development. In early development, this role of Ca^{2+} is well established. Thus so-called fast (10 to 30 μm/second) Ca^{2+} waves are known to restart development during fertilization in metazoa from sponges to man (Jaffe, 1991, 1993); while slow (~1 μm/second) Ca^{2+} waves both accompany and are needed to start and to extend early cleavage furrows in the large eggs of *Xenopus* (Miller et al., 1993; Snow and Nuccitelli, 1993), medaka fish (Fluck et al., 1991) and zebrafish (Chang and Meng, 1995; Webb et al., 1997). Moreover, the segregation of cytoplasm and of oil droplets to the opposite poles of the medaka egg before first cleavage is accompanied and dependent upon the prolonged presence of high Ca^{2+} zones at these poles (Fluck et al., 1992, 1994). Additional roles of Ca^{2+} in axis formation and pattern formation are suggested by studies in fucoid eggs and slime molds. In the exceptionally symmetrical fucoid zygote, formation of a localized, subsurface zone of high, free Ca^{2+} is needed to establish the region of future rhizoidal outgrowth and thus the basal pole of the organism (Speksnijder et al., 1989). In multicellular aggregates of the cellular slime mold, *D. discoideum*, formation of high free Ca^{2+} regions presage future regions of stalk as opposed to spore cell differentiation (Cubitt et al., 1995; Jaffe, 1997).

Most of our knowledge on roles of Ca^{2+} in late vertebrate development comes from the amphibian embryo, in which inhibition or activation of the inositol-Ca^{2+} signaling pathway affects specification of the dorso-ventral axis (Ault et al., 1996; Kume et al., 1997). Moreover, there is very interesting evidence that neural induction in amphibians involves an increase in cytosolic Ca^{2+} via L-type Ca^{2+} channels (Moreau et al., 1994; Drean et al., 1995; Leclerc et al., 1995, 1997). However, Ca^{2+} patterns have never been imaged during long periods in vertebrate development. For example, no Ca^{2+} measurements have been made during regionalization of the vertebrate central nervous system, which depends on various secreted signaling proteins such as WNT-1 and FGF-8 (Bally-Cuif and Wassef, 1995). Perhaps Ca^{2+} plays a role in the secretion of these signaling proteins or in the transduction of the extracellular signal to the nucleus.

In order to directly explore the character and roles of free Ca^{2+} during vertebrate development, we have imaged Ca^{2+} patterns in embryos of the zebrafish, *Danio rerio*, using the luminescent Ca^{2+} indicator aequorin. Aequorin-based Ca^{2+}

imaging is non-disturbing to the embryo allowing continuous imaging during the first days of development. Although it is possible to express apo-aequorin genetically (Rizzuto et al., 1994; Brini et al., 1995), we chose to directly microinject aequorin since this circumvents slow uptake of the aequorin co-factor (Créton et al., 1997). We observed free Ca^{2+} patterns during normal development over 24 hours and thus throughout the cleavage, blastula, gastrula and segmentation periods (Kimmel et al., 1995).

MATERIALS AND METHODS

Zebrafish embryos

A small colony of zebrafish (100 fish in two aquaria) was kept on an artificial 14 hour day/10 hour night cycle at 28.5°C. Fertilized eggs were collected in a spawning cage 30 minutes after 'dawn'. The embryos were kept at 28.5°C in spring water containing 1 mg/l of methylene blue during all measurements up to 24 hours. Afterwards, the embryos were immobilized by adding 1% agarose to this same medium.

Use of aequorin

Zygotes were injected with 2 nl of aequorin dissolved in a buffer containing 100 mM KCl, 0.05 mM EDTA and 5 mM MOPS, pH 7.05, using a high pressure system PLI-100 from the Medical Systems Co., Greenvale, NY 11548 (Miller et al., 1994). We injected either the usual, near natural, recombinant, R-aequorin (at 0.57 mM) or a semi-synthetic recombinant *h*-aequorin (at 0.24 mM); these were kindly provided by Dr Osamu Shimomura. The more sensitive *h*-aequorin was used to image the first 6 hours of development, whereas the longer lasting R-aequorin was used to image Ca^{2+} in later development. With an egg volume of about 200 nl the final aequorin concentrations in the embryo were 5.7 μM for R-aequorin and 2.4 μM for *h*-aequorin. The microinjection needle was pushed through the vegetal regions of the chorion and the plasma membrane to inject the aequorin into the center of the uncleaved egg. However, when focusing on pattern along the animal-vegetal axis, the needle was pushed through the egg's lateral region to avoid vegetal wound signals. The use of aequorins for Ca^{2+} imaging has been reviewed by Miller et al. (1994).

In the course of 25 experiments, we injected approximately 250 embryos with aequorin. From a batch of about ten injected embryos, we typically selected one embryo for Ca^{2+} imaging and one embryo for Ca^{2+} measurements with the photomultiplier tube. In selecting the embryos, we looked for an embryo which had little or no cytoplasm leaking from the injection wound. The injection wounds were visible on the imaging photon detector as high Ca^{2+} regions. Large wounds obscured the Ca^{2+} patterns and decreased embryonic survival. Small wounds healed up quickly (within half an hour) and did not affect embryonic development.

To map the Ca^{2+} patterns during embryonic development, we have measured a total of 25 embryos using the imaging photon detector and 17 embryos using the photomultiplier tube. To calculate the average luminescence and the standard error of the mean (s.e.m.) we used those embryos, which developed normally, were imaged at a specific embryological stage, had the same orientation (side or top-view), and had the same type of aequorin injected (h- or R-aequorin).

Ca^{2+} measurement and imaging

The total level of luminescence versus time was monitored with a Hamamatsu model 464 photomultiplier tube or PMT. The PMT does not provide spatial information, but does provide an overview of Ca^{2+} levels throughout development. PMT values were calibrated to match the output of our imaging system.

Our Ca^{2+} imaging system is based on a Zeiss 100TV axiovert microscope with a 20× fluar objective (NA=0.75). To minimize instrumental noise and allow the recording of data over many hours without overloading memory, we record the dim aequorin light with a so-called Imaging Photon Detector or IPD made by Photek Inc., East Sussex TN389NS, England (reviewed by Miller et al., 1994). This instrument stores data in a computer as a list of photon events, each recorded photon having two horizontal space coordinates and one time coordinate. The two space coordinates identify an individual pixel in the imaging field and with the 20× objective, each pixel corresponded to a specimen area of 10 μm × 10 μm. The digital storage of photons allows flexible reviewing of the Ca^{2+} patterns. Thus images of light emitted over any desired period can be created pointillist style. In general, we first graphed the total luminescence emerging from an embryo against time to detect any peaks in Ca^{2+}. Then, subsequent images of 10 minute photon exposures are analyzed to detect any Ca^{2+} localizations. Whenever a Ca^{2+} peak or Ca^{2+} localization is found, the data is analyzed in more detail, making graphs of specific regions within the embryo and forming images using shorter exposure times. Our imaging system collects data from a wide depth of field along the *z*-axis (at least 200 μm with the 20× objective). To obtain three-dimensional information on Ca^{2+} patterning we routinely imaged developing embryos in various orientations. This wide depth of field also makes the system more sensitive for differences in tissue thickness than for instance a confocal imaging system would. To control for such differences we consistently compared embryonic regions of equal thickness.

In order to determine Ca^{2+} pulse frequencies, we needed to distinguish genuine pulses from statistical fluctuations. To do this, we compared the time course of luminescence from developing embryos to that from BAPTA buffered droplets containing comparable levels of free Ca^{2+} and of aequorin. A Ca^{2+} pulse was defined as an increase in luminescence which was twice the resting level since such fluctuations were never seen in the droplet dummies.

To control for differential distribution or consumption of aequorin, we added 0.1 ml of 10% Triton to the water surrounding the embryo at the end of a typical experiment. The Triton treatment causes a massive increase in cellular Ca^{2+} and 'burns out' the aequorin still present. These burnouts indicated that the aequorin was still evenly distributed in the embryos and that little decay of the aequorin had occurred.

Calibration of the imaging system

The IPD system was calibrated using BAPTA buffers in which free Ca^{2+} was set at specific concentrations. The BAPTA buffers contained either 5.7 μM R-aequorin or 2.4 μM *h*-aequorin in 100 mM KCl, 10 mM monopotassium Hepes, pH 7.0, 1 mM $MgCl_2$, 5 mM tetrapotassium BAPTA and either 1.0 mM, 1.6 mM, 2.4 mM or 3.2 mM $CaCl_2$ to set the free Ca^{2+} concentration at 50, 100, 200 or 400 nM (Pethig et al., 1989). Immediately after adding aequorin, 0.2 μl of the luminescent buffer was injected as a spherical droplet under halocarbon oil. The luminescent spheres were imaged on the IPD, using the 20× objective as if they were eggs.

Fig. 1 shows the result of this calibration. We measured 6.7 times more light with *h*-aequorin at a 2.4 times lower concentration. This 16-fold ratio (6.7 × 2.4) in sensitivities of R and of *h* aequorins corresponds well to the figure reported earlier by Shimomura et al. (1993). The luminescence of both R- and *h*-aequorin rises with the 2.1 power of free Ca^{2+} over the mid range needed to interpret spike heights from developing embryos. This is the same power recently reported by Shimomura and Inouye (1996).

Ca^{2+} clamping and damping in the embryo

To clamp the Ca^{2+} level in the embryo, we injected high concentrations of a Ca^{2+} buffer, in which the free Ca^{2+} concentration was set at pCa 7 (or 100 nM). The Ca^{2+} buffer contained 250 mM tetrapotassium BAPTA, 81 mM $CaCl_2$ and 10 mM Tris, pH 7.5. With an injection volume of 1 nl, the final cytosolic concentration of BAPTA was estimated to be about 2.5 mM (assuming that half of the

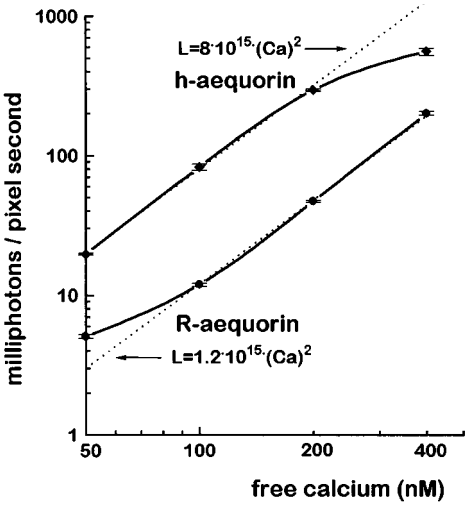

Fig. 1. Calibration of aequorin luminescence with known concentrations of free Ca^{2+}. The Ca^{2+} concentration (Ca) can be calculated from the luminescence (L) using the equations or the curves in the graph. The equations are represented by dotted lines and are only valid for the range in which they overlap with the calibration curve. The exponential portions of both curves show luminescence rising with the 2.1 power of free Ca^{2+}.

egg volume is non-cytosolic). As a control we injected 1 nl of a Tris-buffered, pH 7.5, KCl solution, which was isotonic to the BAPTA buffer. To dampen Ca^{2+} changes in the embryo, we injected the same BAPTA buffer at a five times lower concentration, thus giving a final cytosolic BAPTA concentration of approximately 0.5 mM.

RESULTS

An overview of Ca^{2+} signals during embryonic development

Fig. 2 shows a representative record of total luminescence versus time from a whole, normally developing embryo during the first day and thus up to the end of the segmentation period. It shows increasing levels of luminescence and hence of free cytosolic Ca^{2+} during three main periods: first, during each of the first 5 relatively synchronous cleavages in the period between 0.7 and 2.0 hours. Second, during specification of the dorso-ventral axis and the beginning of gastrulation from about 4 to 7 hours. Third, from about 10 to 13 hours during early segmentation. In addition to relatively slow changes in Ca^{2+}, Fig. 2 shows numerous Ca^{2+} spikes which appear as vertical lines on this time scale. All of these vertical lines represent discrete Ca^{2+} signals rather than noise. These brief signals become larger and more frequent after about 10 hours when segmentation starts.

The three periods of Ca^{2+} elevation and the late Ca^{2+} spikes shown in Fig. 2 were similar in all of the embryos studied (n=9 for 0.5-2 hours, n=7 for 2-3 hours, n=6 for 3-22 hours). Thus the relative changes in luminescence were essentially the same in all embryos; however, the absolute levels of luminescence covered a fourfold range in different embryos. This considerable range in absolute luminescence was probably due to variability in microinjection volume, in the amount of aequorin burned up by Ca^{2+} leakage during injection, as well as variability in Ca^{2+} levels from embryo to embryo. To estimate the total amount of aequorin present in each of the embryos, we burned out all of the available aequorin after 24 hours of development. These burnouts averaged 72 million photons for R-aequorin (±36, n=4). By comparing these burnouts with the total luminescence emitted during development, we calculated that 71% of the injected aequorin was still present after 24 hours of development (±9%, n=3). This corresponds to an in vivo half-life of R-aequorin of 48 hours. The ultra sensitive *h*-aequorin is expected to decay 16× faster (Shimomura et al., 1993), and was thus used for Ca^{2+} imaging during early development only (0-6 hours).

Ca^{2+} patterns during the cleavage period

Ca^{2+} patterns during the cleavage period were imaged using the ultra-sensitive h-aequorin. The earliest imageable luminescence (at half an hour after fertilization) was uniformly

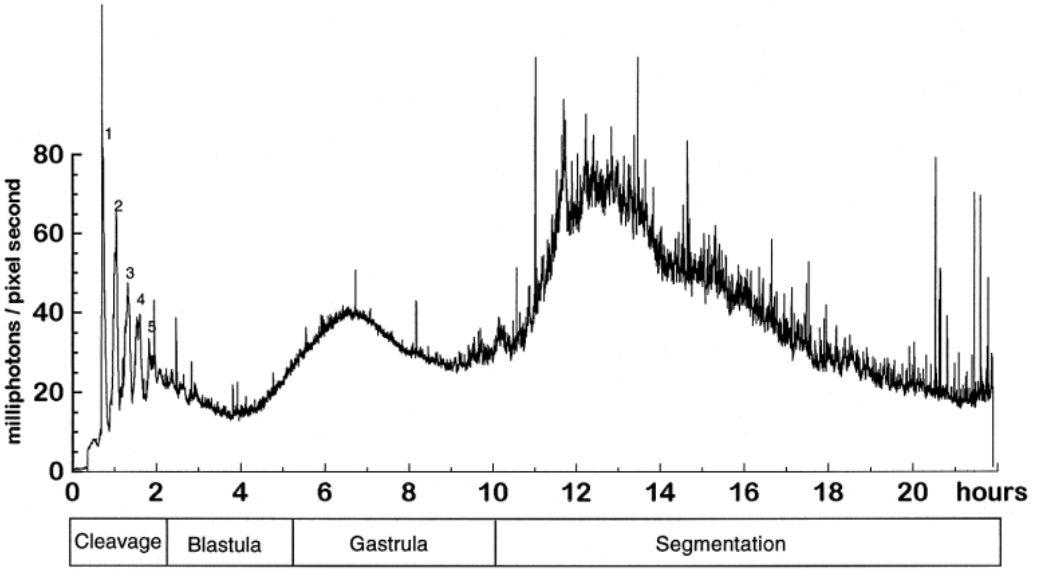

Fig. 2. Representative time course of luminescence from an R-aequorin injected zebrafish embryo during the first 22 hours of development. The inferred average Ca^{2+} level cycles during the first five cycles (0.75-2 hours) and is elevated during mid-gastrulation (6-8 hours) and early segmentation (11-16 hours). Note the greatly increased frequency of Ca^{2+} spikes after 10 hours. The emitted light was measured with a photomultiplier tube.

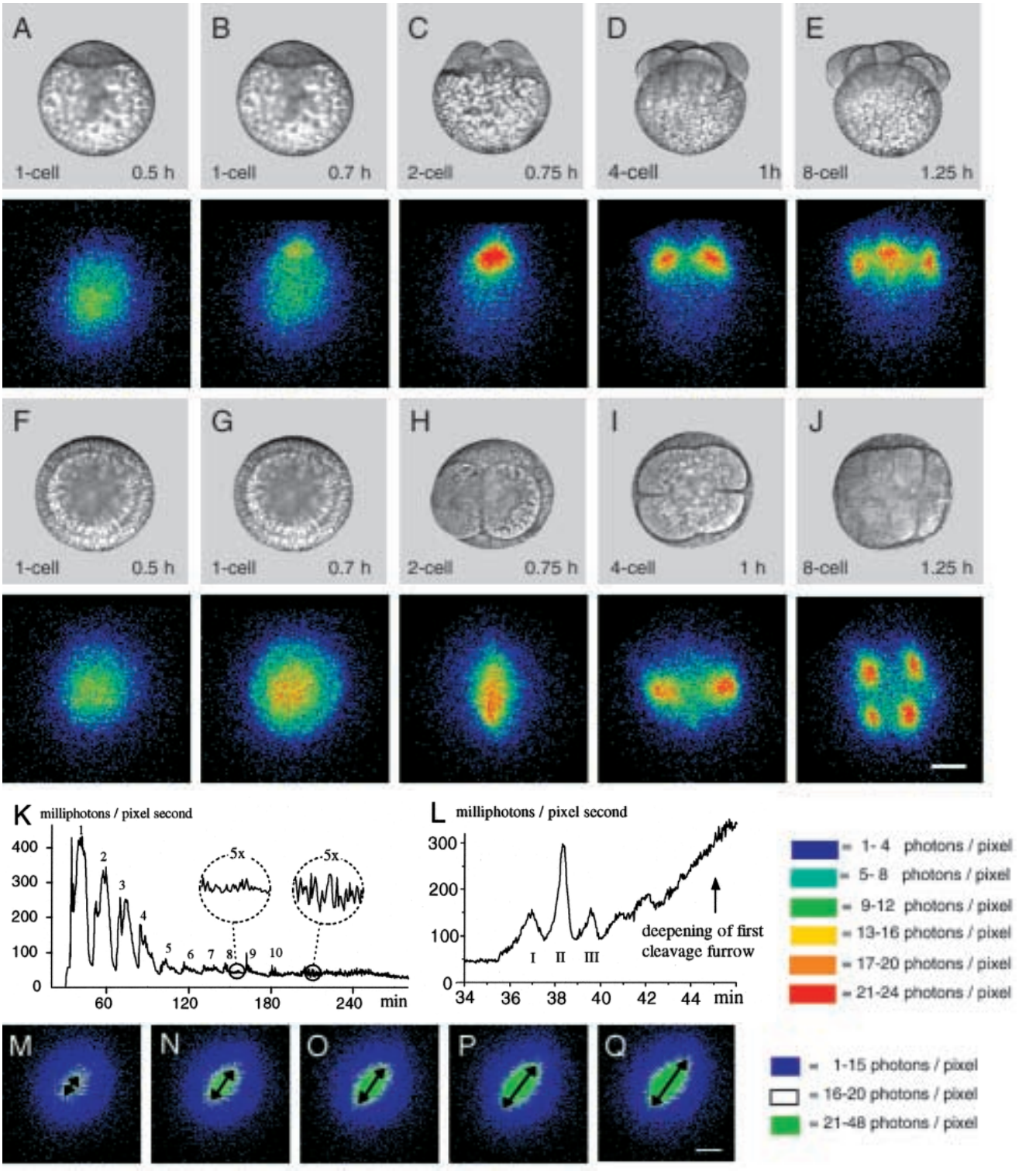

Fig. 3. Representative Ca^{2+} patterns during early cell division obtained by using the ultra-sensitive *h*-aequorin. (A-E) Side views in the median focal plane. (F-J) Top views with focal plane 30% down from the animal pole. High Ca^{2+} is seen at the sites of cytokinesis. The images (A-J) are 30,000 photon exposures (~ 1 minute), in which the level of luminescence was color-coded, red representing high Ca^{2+}, blue representing low Ca^{2+}. (K) Graph showing Ca^{2+} levels during the early cleavage cycles. Cleavage signals can be observed up until the 10^{th} cleavage cycle. From 3.5-4.5 hours of development, small spikes are seen which clearly exceed the noise levels shown between cycles 8 and 9. (L) Three peaks were observed during first cleavage initiation. The arrow indicates the time of furrow deepening. (M-Q) Subsequent 50 second exposures show that the Ca^{2+} elevation during furrow deepening spreads as a slow wave (0.5 μm/second) along the cleavage furrow. Bars, 200 μm.

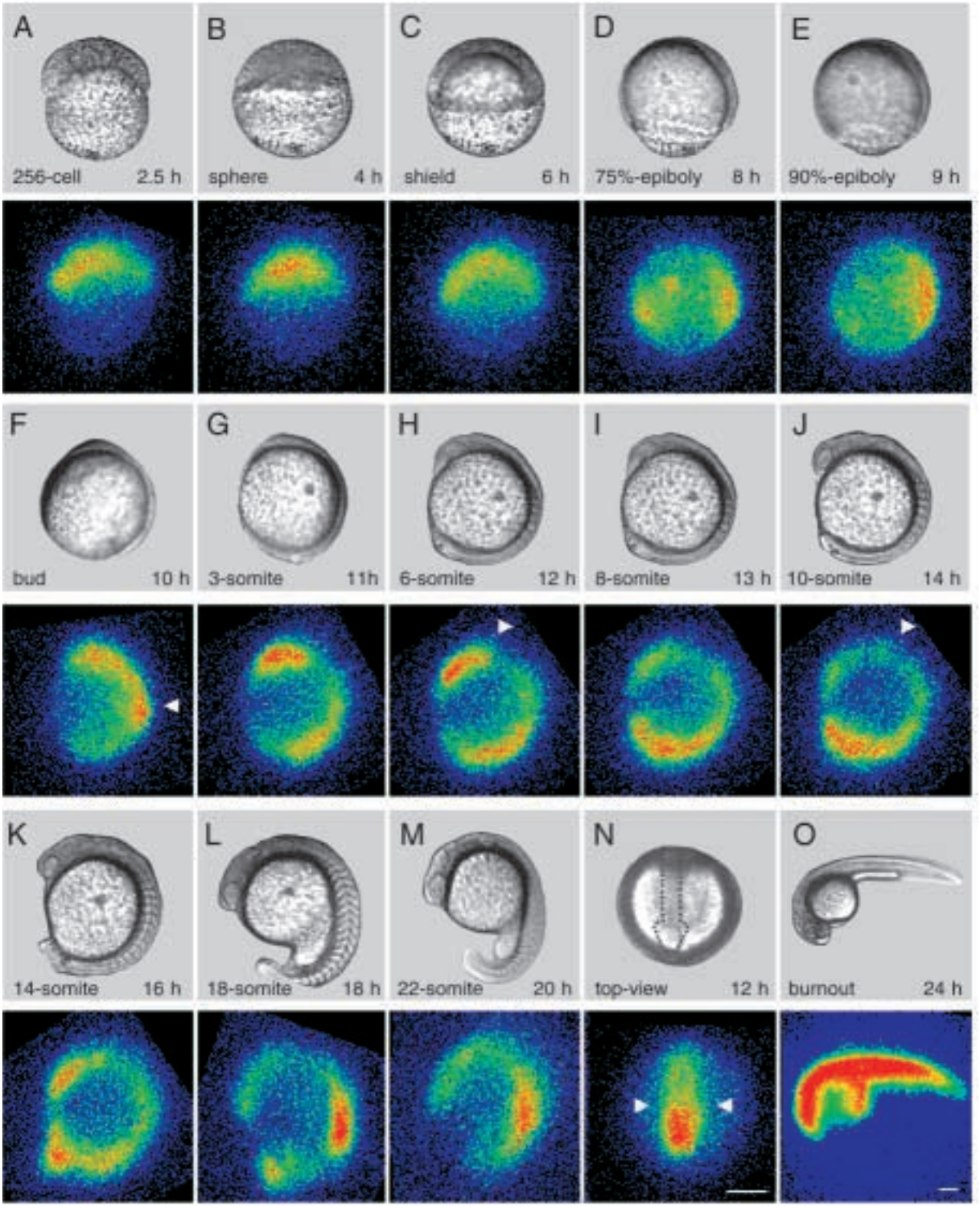

Fig. 4. Ca^{2+} patterns in the blastula, gastrula and segmentation periods. (A-C) The overall Ca^{2+} pattern is uniform within the cellular region of the blastula and early gastrula. (D-F) At 75% epiboly (8 hours), luminescence is high in the blastoderm margin, with peak levels in the dorsal blastoderm margin. Dorsal luminescence becomes stronger and spreads anteriorly in the period from 8 to 10 hours. In the bud stage, a high Ca^{2+} region (arrowhead) appears at about the location of the forming first somite. From the 3 somite through the 14 somite stage (G-K), this high Ca^{2+} region accompanies the tailward formation of additional somites together with the tailward elongation of the neural keel. During and beyond this same period, a remarkable low Ca^{2+} region appears and remains in the future hindbrain region. Note the sharp Ca^{2+} boundary at about the midbrain/hindbrain border arrowed at the 6-somite stage in H and N. (The top view shown in N also shows that the high Ca^{2+} in the front is not coming from the eye primordia.) Also note the small high Ca^{2+} region arrowed in J which probably represents formation of the otic placode. The high Ca^{2+} regions at the 18-22 somite stages (L-M) probably arise from early muscle movements. Images are 30,000 photon exposures. Bars, 200 μm.

distributed (Fig. 3A,F) and averaged 25 (±10, *n*=5) milliphotons per pixel second (mp/ps). This resting level corresponds to approximately 60 nM free Ca^{2+} (Fig. 1). Then, in the first five minutes of first cleavage initiation, Ca^{2+} elevates at the animal pole of the egg (Fig. 3B). During this first cleavage initiation period, three distinct peaks are seen (Fig. 3B,G,L). These three peaks average 69 (±31, *n*=5), 108 (±60, *n*=5), and 74 (±32, *n*=5) mp/ps, corresponding to approximately 90, 120, and 100 nM free Ca^{2+} (for calibration see Fig. 1). We could see these initiation signals with *h*-aequorin, but could not see them with the less sensitive R-aequorin, nor were they seen with Ca^{2+} green dextran by Chang and Meng (1995).

Large rises of Ca^{2+} are seen within the deepening furrow during each of the first three cleavages (Fig. 3C-E, H-J). During the first cleavage, this rise begins near the central nuclei, reaches a peak of 360 mp/ps (±140, *n*=5) corresponding to a peak level of about 250 nM free Ca^{2+} and spreads outwards at 0.5 μm/second (Fig. 3M-Q). Although cleavage signals can be observed up until the 10th cleavage (Fig. 3K), the total luminescence generated by all of the synchronous cleaving blastomeres becomes smaller in later cell divisions (Fig. 2).

Ca^{2+} patterns in blastula and gastrula stages

Small spikes were generated at a frequency of about one per minute between 3.5 and 4.5 hours during the blastula stage (Fig. 3K). These spikes were most apparent when using *h*-aequorin, but could also be observed using R-aequorin. The overall Ca^{2+} pattern is uniform within the cellular region of the blastula and early gastrula (Fig. 4A-C). However, in four out of seven embryos, we observed higher Ca^{2+} in the presumptive ventral region than in the presumptive dorsal one from 2.5-3 hours of development. (The dorso-ventral axis was determined retrospectively, by videotaping embryos up until 6.5 hours of development.) We did not pursue this Ca^{2+} gradient, since one of the seven embryos showed a reverse Ca^{2+} gradient, while the two remaining embryos showed uniform Ca^{2+} patterns from 2.5-3 hours of development.

At 75% epiboly (8 hours), luminescence is high in the blastoderm margin, with peak levels in the dorsal blastoderm margin (Fig. 4D). Dorsal luminescence becomes stronger and spreads forwards (in anterior direction) from the organizer region at about 0.05 μm/second from 8 to 10 hours (Fig. 4D-F).

The segmentation period; Ca^{2+} patterns in the head region

At 10-11 hours of development, distinct Ca^{2+} patterns can be recognized along the antero-posterior axis of the embryo (Fig. 4F,G). Most apparent is the high Ca^{2+} zone which appears in the presumptive fore and midbrain regions in contrast to the presumptive hindbrain region. The presumptive hindbrain of a 10-hour old embryo consists of a small area that is laterally stretched over the blastoderm. The lengthening of the low Ca^{2+} zone seen from 10 to 14 hours in Fig. 4F-J probably corresponds to the elongation of the future hindbrain during this same period (Woo and Fraser, 1995). The Ca^{2+} elevation in the anterior head region becomes more pronounced at 12 hours of development (Fig. 4H). At this point, the mid- and forebrain luminesce 1.7 times (±0.3, *n*=4) brighter than the hindbrain. This corresponds to a Ca^{2+} concentration of 144 nM in the mid- and forebrain and 112 nM in the hindbrain (see Fig. 1 for calibration). A relative sharp border separates elevated Ca^{2+} in the presumptive mid- and forebrain from low Ca^{2+} in the presumptive hindbrain. At 14 hours, the low level of Ca^{2+} in the hindbrain is locally interrupted by an elevation of Ca^{2+} which is associated with the formation of the otic placode (Fig. 4J). The overall luminescence remains 1.7 times (± 0.2, *n*=4) higher in the forebrain as compared to the hindbrain. Even at 16 hours of development, Ca^{2+} remains low in the hindbrain region. Ca^{2+} patterns were also studied in embryos viewed from the top. Again, the most striking feature was the midbrain-hindbrain border, with high Ca^{2+} in the fore and mid brain and low Ca^{2+} in the hindbrain (Fig. 4N).

An important control in Ca^{2+} imaging with aequorin is the burnout, which shows whether or not aequorin was uniformly distributed throughout the embryo (Fig. 4O). For the burnout, Triton is added to the culture medium creating holes in the plasma membranes. Intracellular Ca^{2+} levels quickly rise to the millimolar range and all of the aequorin burns up. From these burnout experiments we learned that aequorin concentrations are low in the yolk region. Probably very little of the cytosol (which contains aequorin) is present between the densely packed yolk granule. Thus, the low luminescence observed in the yolk area during embryonic development may be simply due to a lack of aequorin. In contrast, aequorin was uniformly distributed in the embryo proper.

The segmentation period; Ca^{2+} patterns in the trunk and tail

The trunk region develops a higher Ca^{2+} zone than the adjoining hindbrain and tail regions. This zone moves backwards to the tip of the tail from about 10 to 14 hours at 0.07 μm/second (Fig. 4F-J). At 14-16 hours, Ca^{2+} appears as a gradient along the antero-posterior axis, with the highest Ca^{2+} concentrations in the tip of the tail. Thus, an ultraslow Ca^{2+} wave moves posteriorly along with the formation of the somites and neural keel.

At 14 hours, the trunk emits 1.8 times (±0.3, *n*=4) more luminescence than the hindbrain. The tail emits 2.4 times (±0.7, *n*=4) more luminescence than the hindbrain. This corresponds to a Ca^{2+} concentration of 86 nM in the hindbrain, 115 nM in the trunk region, and 133 nM in the tail region. At 18 hours, the tail of the embryo starts moving and high Ca^{2+} is observed in the region of the embryo showing spontaneous muscle contractions. A similar Ca^{2+} signal is observed in the tail region of the embryo at 20 hours of development (Fig. 4M).

The segmentation period; Ca^{2+} spikes

Starting at 11 hours of development, a radical increase in the frequency of Ca^{2+} spikes is seen (Fig. 2). From 12 to 22 hours embryos generate about 80 spikes. The 12 hour embryos averaged 8.5 spikes per hour (±4, *n*=4) and the 14 hour embryos averaged 8.0 spikes per hour (±2, *n*=3).

The duration of the spikes ranges from 10 to 200 seconds and the increase in luminescence has a doubling time ranging between 1 and 40 seconds (Fig. 5). The vast majority of the spikes (96%) are present in the hindbrain, trunk and tail region (approximately 32% each). Only 4% (±3, *n*=7) of the spikes are localized in the head region even though it represents the most anterior 25% of the embryo. Thus the spike frequency in the head region is extremely low - on average only one spike

per three hours. Moreover, the pulses in the head region were small as well, increasing the levels of luminescence by only a two to four fold (Fig. 5A). Ca^{2+} spikes may be far more important in other embryonic regions particularly the hindbrain and the heart where the pulses occur far more frequently and are much larger. For example, spikes from the heart are observed every 10-20 minutes and the level of luminescence increases up to a 100-fold (Fig. 5E,F). This 100-fold increase in luminescence corresponds to approximately a 10-fold increase in Ca^{2+} concentration, suggesting that the Ca^{2+} concentration in the heart is temporarily raised to the micromolar range.

Ca^{2+} buffering with BAPTA

To block normal Ca^{2+} patterning during cleavage, we injected the Ca^{2+} buffer BAPTA into uncleaved zygotes to yield a final BAPTA concentration in the cytosol of about 2.5 mM. These embryos did not cleave and remained in the one cell stage until they lysed (data not shown). In some cases, they survived for more than 24 hours without any sign of development.

When lower concentrations of BAPTA were injected (0.5 mM final concentration in the cytosol), the embryos developed into fish having several developmental defects (Fig. 6). The most apparent defect was the deformation of the heart. Although an atrium and a ventricle were formed within the heart, the heart remained small and was usually not capable of pumping blood. A large pericardium formed around the heart and the heart was stretched in the longitudinal direction.

A second defect observed in such BAPTA injected embryos was a reduction in eye size. The eyes of the BAPTA injected embryos were measured after 4 days and averaged 182 μm in diameter (±4, *n*=9). The eyes of the control embryos averaged 320 μm in diameter (±3, *n*=16), and were therefor 1.8× wider and 6× larger in volume. In contrast, the otic placodes of the BAPTA injected embryos were not significantly reduced in size. The otic placodes of the BAPTA-injected embryos averaged 193 μm (±3, *n*=9) and the ones of the control embryos averaged 200 μm (±2, *n*=16). The BAPTA-induced reduction of eye size can not be explained by a simple delay of development. This because younger control embryos have small eyes, but have small otic placodes as well. For example, a 24-hour-old control embryo has an average eye size of 205 μm (±4, *n*=12) and an otic placode size of 86 μm (±3, *n*=12). Apart from the heart and eye defects, such BAPTA injected embryos developed fairly normally according to gross morphological criteria. For example, the embryos had blood cells, somites, a brain, pigmentation in the retina, a lens in the eye, fins, and showed muscle movements and a touch reflex. Such BAPTA-injected embryos were usually a bit smaller than the controls and in the more severe cases they had short tails.

DISCUSSION

The cleavage period

Ca^{2+} signals associated with cleavage have been previously measured in medaka and zebrafish eggs (Fluck et al., 1991; Chang and Meng, 1995; Webb et al., 1997). Our results support these earlier observations. Moreover, we have measured additional Ca^{2+} peaks in the first five minutes of cleavage initiation.

At the onset of first cleavage we observed three distinct Ca^{2+} peaks. The second, and largest, of the three cleavage initiation peaks probably corresponds to the 'furrow propagation signal', which is a Ca^{2+} wave associated with the furrow elongation as described in zebrafish embryos (Webb et al., 1997). A similar Ca^{2+} signal or 'furrowing wave' has also been shown in medaka fish embryos (Fluck et al., 1991). The role of the two additional Ca^{2+} signals (the first and third initiation signal) remains to be determined. Judging from observations on sea urchin and amphibian eggs the first of these Ca^{2+} signals may function in nuclear envelope breakdown (Browne et al., 1996; Wilding et al., 1996), chromosome disjunction (Groigno and Whitaker, 1998), surface contraction (Hara, 1971), or furrow positioning (Miller et al., 1993; Webb et al., 1997).

During the subsequent deepening of the cleavage furrow we observed a Ca^{2+} wave which spreads at a velocity of 0.5 μm/second. It has been previously suggested that similar slow Ca^{2+} waves cause growth of furrowing membranes by means of exocytosis and are required for 'zipping' the blastomeres together (Fluck et al., 1991). Another possible role of high furrow Ca^{2+} is to localize cytoplasmic factors, as previously shown during polarization in fucus eggs (Speksnijder et al., 1989) and during ooplasmic segregation in medaka fish eggs (Fluck et al., 1994). Interestingly, a germ-cell-specific marker (vas RNA) localizes to the cleavage plane in 2- and 4-cell stage zebrafish embryos (Yoon et al., 1997). The speed of the Ca^{2+} waves during furrow deepening (0.5 μm/second), corresponds well with observations in medaka in which both the furrowing and zipping waves move at 0.5 μm/second (Fluck et al., 1991). Moreover, the data of Webb et al. (1997) do show furrowing and deepening waves with velocities of 0.5 and 0.5 to 0.7 μm/second, respectively. These cleavage waves are believed to be members of a large and distinct class of slow Ca^{2+} waves with conserved speeds (Jaffe, 1993).

Strong evidence that Ca^{2+} is needed for cleavage is provided by the results of Ca^{2+} buffer (BAPTA) injection into *Xenopus* (Miller et al., 1993; Snow and Nuccitelli, 1993), and zebrafish eggs (Chang and Meng, 1995; Webb et al., 1997). In our hands, a final cytosolic concentration of 2.5 mM BAPTA can completely block development for up to 24 hours. A similar effect was previously observed in fucoid eggs, some of which respond to comparable Ca^{2+} buffer injections by suspending visible development for ten days or more (Speksnijder et al., 1989).

The blastula and gastrula period

The first sign of Ca^{2+} signaling during the blastula period is an increase in spike frequency at 3.5 hours after fertilization. One might imagine that these small spikes reflect the asynchronous divisions of relatively small cells. However, a detailed study of Ca^{2+} spikes in the zebrafish blastula (done with a fluorescent reporter) showed comparable signals that are restricted to the outermost or EVL cells, that often occur within single cells at more than 10 times per hour and that occur at times which are not correlated with the cell cycle (Reinhard et al., 1995). Thus, the blastula spikes are not likely to be cell division signals. The observed increase in spike frequency might indicate the activation of a particular signal transduction pathway. The spike frequency in the enveloping layer can for example be doubled by expression of Xwnt-5A in zebrafish embryos (Slusarski et al., 1997). Moreover, endogenous IP3 levels are

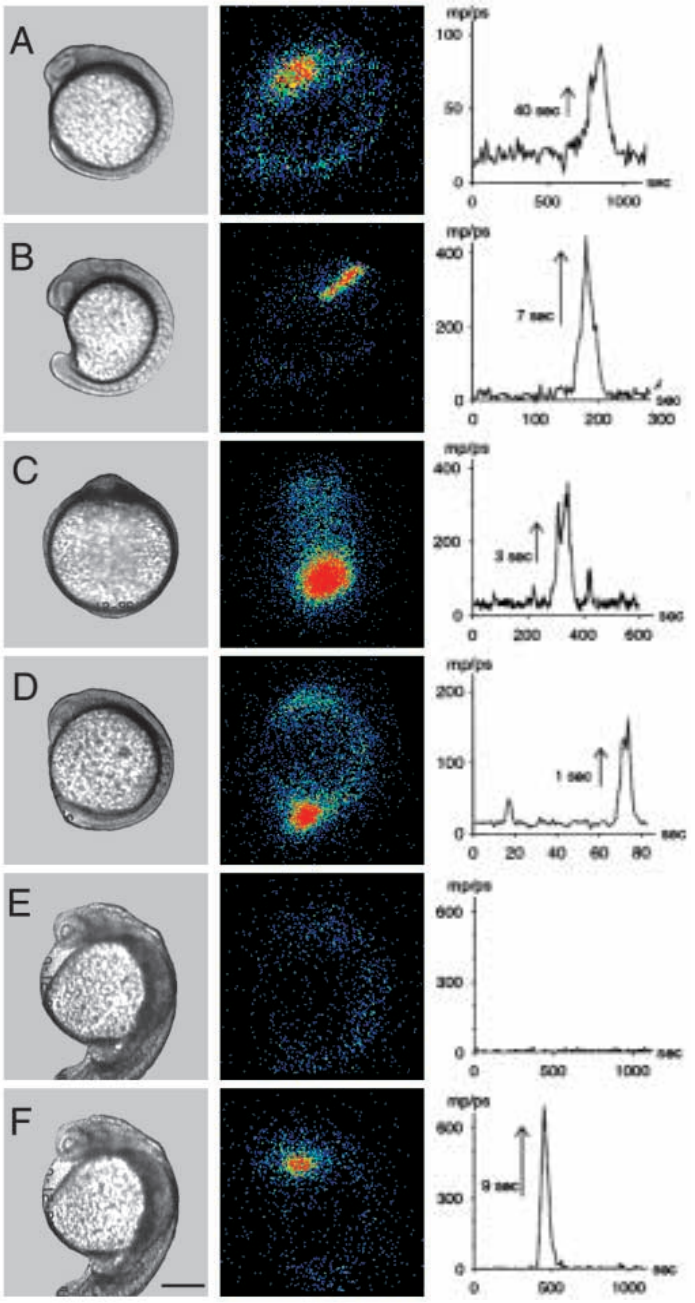

Fig. 5. Ca^{2+} spikes appear from 11 hours onwards. These spikes are very rarely seen in the future head (A) but appear at a frequency of about 8 times per hour in the future hindbrain (B), trunk (C; top view) and tail (D) from 11 to 22 hours. Ca^{2+} pulses are not observed in the heart region at 26 hours (E) but are seen at 28 hours (F). These huge (!) spikes appear every 10 to 20 minutes for several hours. Numbers next to upward arrows in the graphs indicate luminescence doubling times. Images are 30,000 photon exposures, Bar, 200 μm.

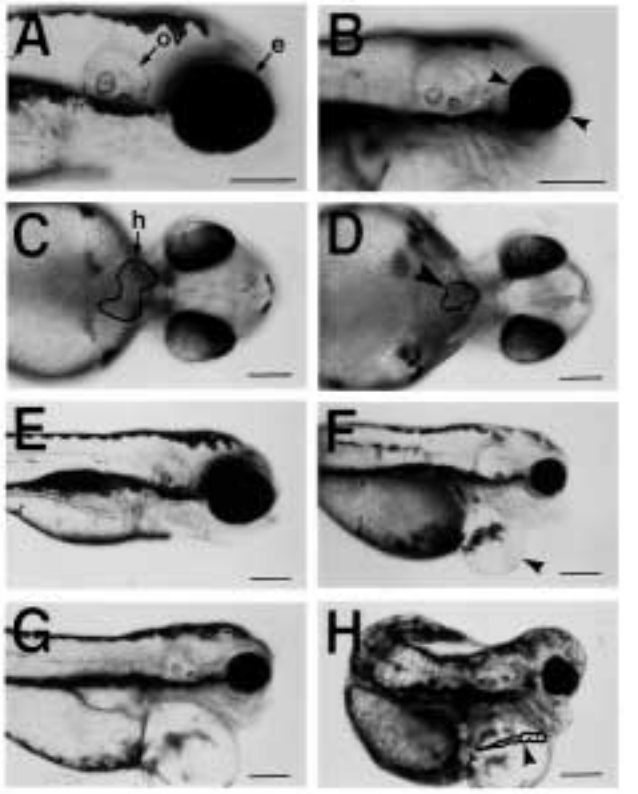

Fig. 6. Embryonic defects after injection of the Ca^{2+} buffer BAPTA. The pictures show 4-day-old embryos as observed with transmitted light microscopy. (A) Control embryo: the size of the eye (e) and otic vesicle (ov) were measured along the antero-posterior axis. (B) BAPTA-injected embryos have reduced eyes (arrowheads). The size of the otic vesicle is not affected by BAPTA injection. (C) Control embryo ventral view, showing the heart (h). (D) The BAPTA injected embryos have small hearts. (E) Control embryo at lower magnification. (F,G) The majority of the BAPTA-injected embryos have a pouch around the heart (arrowhead). (H) Approximately 5% of the BAPTA-injected embryos has a more severe phenotype, with a shortened antero-posterior axis and a deformed heart, which is outlined on the picture (arrowhead). This heart contracts but is incapable of pumping blood. Bars, 100 μm.

substantially elevated at 3-4 hours after fertilization (Reinhard et al., 1995).

In the late blastula stage, the total level of free Ca^{2+} increases (Fig. 2). This increase starts at a time coincident with the first indicators of organization along a second axis, namely *goosecoid* expression (Stachel et al., 1993) followed by blastoderm thinning (Schmitz and Campos-Ortega, 1994) and endocytosis (Cooper and D'Amico, 1996) in the dorsal region. The level of free Ca^{2+} reaches a maximum during early gastrulation (6.5 hours), when epiboly resumes and the embryonic shield starts to extend towards the animal pole.

At 75% epiboly (8 hours), luminescence is high in the blastoderm margin, with peak levels in the dorsal blastoderm margin. Dorsal luminescence becomes stronger and spreads in the anterior direction from 8 to 10 hours. While this anterior spread does suggest a corresponding, ultraslow Ca^{2+} wave, it may only indicate extension of a thicker embryonic region. Our imaging method fails to distinguish between these possibilities. However, observations of a 0.1 μm/second surface contraction wave spreading along a comparable path during primary neural induction in the axolotl (Brodland et al., 1994) suggest that our luminescence wave may partly reflect a slow Ca^{2+} wave. So does evidence which indicates that neural induction in amphibians involves an increase in cytosolic Ca^{2+} within the

ectoderm via an influx of Ca^{2+} from extracellular regions (Moreau et al., 1994; Drean et al., 1995; Leclerc et al., 1995, 1997).

The segmentation period

At 10-11 hours of development, distinct Ca^{2+} patterns can be recognized along the antero-posterior axis of the embryo. High Ca^{2+} was observed in the presumptive mid- and forebrain in contrast to low Ca^{2+} in the presumptive hindbrain. This striking Ca^{2+} pattern in the brain remains clearly visible for several hours and precedes morphological patterning of the brain. Morphological segmentation of the zebrafish brain is first apparent at 11 hours of development when eye primordia are formed from the lateral walls of the presumptive forebrain. However, the classical division into forebrain, midbrain and hindbrain is first morphologically obvious at 16 hours of development. We propose that the observed Ca^{2+} patterns help regionalize the central nervous system. The boundary between high and low Ca^{2+} may be involved in formation of the midbrain/hindbrain boundary and high Ca^{2+} itself may be required for rostral differentiation. This idea is supported by the BAPTA-induced reduction of eye size. Since the eyes are formed from the lateral walls of the diencephalon, the reduction in eye size points towards a role of Ca^{2+} in diencephalon development.

Which Ca^{2+}-mediated pathways could possibly underlie brain regionalization? We can imagine at least two roles of Ca^{2+} in brain regionalization: (1) Ca^{2+} may activate transcription, as it does in other neural systems (Ghosh and Greenberg, 1995; Ginty, 1997; Hardingham et al., 1997). It thus seems possible that the rostral high Ca^{2+} zone induces the transcription of rostral-specific genes. Possible target genes are zebrafish versions of orthodenticle which are expressed in the presumptive forebrain and midbrain of zebrafish embryos (Li et al., 1994; Mercier et al., 1995). These so-called *Otx* or *zOtx* genes have a sharp posterior limit of expression at the midbrain-hindbrain border from 10-30 hours of development. (2) Ca^{2+} is known to control secretion in a variety of cellular systems and might thus regulate secretion of extracellular proteins in the brain as well. The process of secretion could in turn be important in brain regionalization, since the formation of the midbrain-hindbrain border depends on secreted proteins such as WNT-1 and FGF-8 (Bally-Cuif and Wassef, 1995; Kelly and Moon 1995; Joyner, 1996; Lee et al., 1997).

Apart from the Ca^{2+} patterns in the head, various Ca^{2+} waves, gradients, and spikes were observed in the trunk and tail region. The most pronounced is an ultraslow Ca^{2+} wave moving posteriorly along with the formation of the somites and neural keel (10-14 hours). Although Ca^{2+} is known to mediate cellular contractions, it remains to be shown whether intracellular Ca^{2+} plays a role in large scale morphogenetic movements such as infolding of the neural keel and formation of the somitic furrows.

The highest Ca^{2+} levels during embryonic development were observed in the spikes. Such high Ca^{2+} may be related to rapid changes in cell morphology or apoptosis. The most pronounced Ca^{2+} spikes were the ones imaged in the heart. These low-frequency high-amplitude spikes are first observed at about 27 hours of development and thus seem to be unrelated to the heart beat, which starts to beat at a rate of 25 beats per minute at 22 hours of development (Stainier et al., 1993). The timing of these Ca^{2+} signals shows a closer correlation with separation of the heart chambers (24-30 hours) or with looping of the heart, which occurs at between 30 and 36 hours of development (Stainier et al., 1993; Fishman and Chien, 1997). The heart defects observed after BAPTA injection suggest that Ca^{2+} signaling is needed for heart growth and development. Defects in the embryonic heart may act back on further heart development, as suggested by studies in the zebrafish mutants *sih*, *web*, *str*, *pip*, and *hip*. The heart shape in these mutant embryos is often distorted (small, stretched, pipe-like) as a result of failing function (Chen et al., 1996).

Future prospects

In the present study we imaged Ca^{2+} patterns in the zebrafish embryo from the uncleaved egg to a small moving fish larva. We did not provide a high resolution picture of each of the Ca^{2+} signals, but rather aimed for an overview. This overview can be used as a guide for Ca^{2+} inhibition studies and for high resolution studies using confocal Ca^{2+} imaging with fluorescent indicators. Confocal Ca^{2+} imaging has already resulted in detailed knowledge of neural activity in post-hatching zebrafish embryos (O'Malley et al., 1996; Fetcho et al., 1997) and seems a promising approach to study specific Ca^{2+} signals in zebrafish development with greater spatio-temporal detail. Moreover, the large number of mutant zebrafish that has become available, will provide a unique opportunity to study how specific genes affect the Ca^{2+} patterns. For instance, do mutant embryos in which the midbrain hindbrain boundary is affected, e.g. *ace* and *noi* (Brand et al., 1996), have altered Ca^{2+} patterning in the brain? Or are Ca^{2+} spikes inhibited in mutant embryos with defective heart development? And if so, would it possible to rescue these mutants by manipulation of Ca^{2+} patterns?

We thank Drs Osamu Shimomura, Satoshi Inouye, and Yoshito Kishi for generously providing the aequorins. This work was supported by the Netherlands Organization for Scientific Research (NWO), the Bernard and Celia Jaffe memorial fund, and a Spiegel fellowship. J.E.S. was supported by a NATO grant (CRG 940244), and by the EC-HCM grant CHRX-CT 940646.

REFERENCES

Ault, K. T., Durmowicz, G., Galione, A., Harger, P. L. and Busa, W. B. (1996). Modulation of *Xenopus* embryo mesoderm-specific gene expression and dorsoanterior patterning by receptors that activate the phosphatidyl-inositol cycle signal transduction pathway. *Development* **122**, 2033-2041.

Bally-Cuif, L. and Wassef, M. (1995). Determination events in the nervous system of the vertebrate embryo. *Curr. Opin. Gen. Dev.* **5**, 450-458.

Brand, M., Heisenberg, C. P., Jiang, Y. J., Beuchle, D., Lun, K., Furutani-Seiki, M., Granato, M., Haffter, P., Hammerschmidt, M., Kane, D. A., Kelsh, R. N., Mullins, M. C., Odenthal, J., van Eeden, F. J. and Nusslein-Volhard, C. (1996). Mutations in zebrafish genes affecting the formation of the boundary between midbrain and hindbrain. *Development* **123**, 179-190.

Brini, M., Marsault, R., Bastianutto, C., Alvarez, J., Pozzan, T. and Rizzuto, R. (1995). Transfected aequorin in the measurement of cytosolic Ca^{2+} concentration ([Ca^{2+}]c). *J. Biol. Chem.* **270**, 9896-9903.

Browne, C. L., Creton, R., Karplus, E., Mohler, P. J., Palazzo, R. E. and Miller, A. L. (1996). Analysis of the calcium transient at NEB during the first cell cycle in dividing sea urchin eggs. *Biol. Bull.* **191**, 5-16.

Brodland, G. W., Gordon, R., Scott, M. J., Bjorklund, N. K., Luchka, K. B., Martin, C. C., Matuga, C., Globus, M., Vethamany-Globus, S. and Shu, D. (1994). Furrowing surface contraction wave coincident with primary neural induction in amphibian embryos. *J. Morphol.* **219**, 131-142.

Chang, D. C. and Meng, C. (1995). A localized elevation of cytosolic free calcium is associated with cytokinesis in the zebrafish embryo. *J. Cell Biol.* **131**, 1539-1545.

Chen, J. N., Haffter, P., Odenthal, J., Vogelsang, E., Brand, M., van Eeden, F. J. M., Furutani-Seiki, M., Granato, M. Hammerschmidt, M., Heisenberg, C. P., Jiang, Y. J., Kane, D. A., Kelsh, R. N., Mullins, M. C. and Nusslein-Volhard, C. (1996). Mutations affecting the cardiovascular system and other internal organs in zebrafish. *Development* **123**, 293-302.

Cooper, M. S. and D'Amico, L. A. (1996). A cluster of noninvoluting endocytic cells at the margin of the zebrasfish blastoderm marks the site of embryonic shield formation. *Dev. Biol.* **180**, 184-198.

Créton, R., Steele, M. and Jaffe, L. F. (1997). Expression of apo-aequorin during embryonic development; how much is needed for calcium imaging? *Cell Calcium* **22**, 439-446.

Cubitt, A. B., Firtel, R. A., Fischer, G., Jaffe, L. F. and Miller, A. L. (1995). Patterns of free calcium in multicellular stages of *Dictyostelium* expressing jellyfish apoaequorin. *Development* **121**, 2291-2301.

Drean, G., Leclerc, C., Duprat, A. M. and Moreau, M. (1995). Expression of L-type Ca^{2+} channel during early embryogenesis in Xenopus laevis. *Int. J. Dev. Biol.* **39**, 1027-1032.

Fetcho, J. R., Cox, K. J. A. and O'Malley, D. M. (1997). Imaging neural activity with single cell resolution in an intact, behaving vertebrate. *Biol. Bull.* **192**, 150-153.

Fishman, M. C. and Chien, K. R. (1997). Fashioning the vertebrate heart: earliest embryonic decisions. *Development* **124**, 2099-2117.

Fluck, R., Miller, A. L. and Jaffe, L. F. (1991). Slow calcium waves accompany cytokinesis in medaka fish eggs. *J. Cell Biol.* **115**, 1259-1265.

Fluck, R. A., Miller, A. L. and Jaffe, L. F. (1992). High calcium zones at the poles of developing medaka eggs. *Biol. Bull.* **183**, 70-77.

Fluck, R. A., Miller, A. L., Abraham, V. C. and Jaffe, L. F. (1994). Calcium buffer injections inhibit ooplasmic segregation in medaka eggs. *Biol. Bull.* **186**, 254-262.

Ghosh, A. and Greenberg, M. E. (1995). Calcium signaling in neurons: molecular mechanisms and cellular consequences. *Science* **268**, 239-247.

Ginty, D. D. (1997). Calcium regulation of gene expression; isn't that spatial? *Neuron* **18**, 183-186.

Groigno, L. and Whitaker, M. (1998). An anaphase calcium signal controls chromosome disjunction in early sea urchin embryos. *Cell* **92**, 193-204.

Hara, K. (1971). Cinematographic observation of surface contraction waves (SCW) during the early cleavage of axolotl. *Wilh. Roux Arch.* **167**, 183-186

Hardingham, G. E., Chawla, S., Johnson, C. M. and Bading, H. (1997). Distinct functions of nuclear and cytoplasmic calcium in the control of gene expression. *Nature* **358**, 260-265.

Jaffe, L. F. (1991). The path of calcium in cytosolic calcium oscillations: a unifying hypothesis. *Proc. Nat. Acad. Sci.USA* **88**, 9883-9887.

Jaffe, L. F. (1993). Classes and mechanisms of calcium waves. *Cell Calcium* **3**, 736-745.

Jaffe, L. F. (1997). The roles of calcium in pattern formation. In *Dictyostelium: A Model System for Cell and Developmental Biology* (ed. Y. Maeda, K. Inouye and I. Takeuchi), pp 267-277. Tokyo: Universal Academy Press.

Joyner, A. L. (1996). Engrailed, Wnt and Pax genes regulate midbrain-hindbrain development. *Trends Genet.* **12**, 15-20.

Kelly, G. M. and Moon, R. T. (1995). Involvement of Wnt1 and Pax2 in the formation of the midbrain-hindbrain boundary in the zebrafish gastrula. *Dev. Genet.* **17**, 129-140.

Kimmel, C. B., Ballard, W. W., Kimmel, S. R., Ullmann, B. and Schilling, T. F. (1995). Stages of embryonic development of the zebrafish. *Dev. Dynam.* **203**, 253-310.

Kume, S., Muto, A., Inoue, T., Suga, K., Okano, H. and Mikoshiba, K. (1997). Role of inositol 1,4,5,-triphosphate receptor in ventral signaling in Xenopus embryos. *Science* **278**, 1940-1943.

Leclerc, C., Duprat, A. M. and Moreau, M. (1995). In vivo labelling of L-type Ca^{2+} channels by fluorescent dihyudropyridine: correlation between ontogenesis of the channels and the acquisition of neural competence in ectoderm cells from Pleurodeles waltl embryos. *Cell Calcium* **17**, 216-224.

Leclerc, C., Daguzan, C., Nicolas, M. T., Chabret, C., Duprat, A. M. and Moreau, M. (1997). L-type calcium channel activation controls the in vivo transduction of the neuralizing signal in amphibian embryos. *Mech. Dev.* **64**, 105-110.

Lee, S. M. K., Danielian, P. S., Fritzsch, B. and McMahon, A. P. (1997). Evidence that FGF8 signalling from the midbrain-hindbrain junction regulates growth and polarity in the developing midbrain. *Development* **24**, 959-969.

Li, Y., Allende, M. L., Finkelstein, R. and Weinberg, E. S. (1994). Expression of two zebrafish ortodenticle-related genes in the embryonic brain. *Mech. Dev.* **48**, 229-244.

Mercier, P., Simeone, A., Cotelli, F. and Boncinelli, E. (1995). Expression pattern of two otx genes suggests a role in specifying anterior body structures in zebrafish. *Int. J. Dev. Biol.* **39**, 559-573.

Miller, A. L., Fluck, R. A., McLaughlin, J. A. and Jaffe, L. F. (1993). Calcium buffer injections inhibit cytokinesis in *Xenopus* eggs. *J. Cell Sci.* **106**, 523-534.

Miller, A. L., Karplus, E. and Jaffe, L. F. (1994). The use of aequorin for Ca^{2+} imaging. In *Methods in Cell Biology, A Practical Guide to the Study of Ca^{2+} in Living Cells*, vol. 40 (ed. R. Nuccitelli), pp. 305-338. Academic Press, Inc., San Diego, CA.

Moreau, M., Leclerc, C., Gualandris-Parisot, L. and Duprat, A. M. (1994). Increased internal Ca^{2+} mediates neural induction in the amphibian embryo. *Proc. Nat. Acad. Sci. USA* **91**, 12639-12643.

O'Malley, D. M., Kao, Y. H. and Fetcho, J. R. (1996). Imaging the functional organization of zebrafish hindbrain segments during escape behaviors. *Neuron* **17**, 1145-1155.

Pethig, R., Kuhn, M., Payne, R., Adler, E., Chen, T. H. and Jaffe, L. F. (1989). On the dissociation constants of BAPTA-type calcium buffers. *Cell Calcium* **10**, 491-498.

Reinhard, E., Yokoe, H., Niebling, K. R., Allbritton, N. L., Kuhn, M. A. and Meyer, T. (1995). Localized calcium signals in early zebrafish development. *Dev. Biol.* **170**, 50-61.

Rizzuto, R., Brini, M. and Pozzan, T. (1994). Targeting recombinant aequorin to specific intracellular organelles. *Meth. Cell Biol.* **40**, 339-354.

Schmitz, B. and Campos-Ortega, J. A. (1994). Dorso-ventral polarity of the zebrafish embryo is distinguishable prior to the onset of gastrulation. Roux's Arch. *Dev. Biol.* **203**, 374-380.

Shimomura, O., Musicki, B., Kishi, Y. and Inouye, S. (1993). Light-emitting properties of recombinant semisynthetic aequorins and recombinant fluorescein-conjugated aequorin for measuring cellular calcium. *Cell Calcium* **14**, 373-378.

Shimomura, O. and Inouye, S. (1996). Titration of recombinant aequorin with calcium chloride. *Biochem. Biophys. Res. Commun.* **221**, 77-81.

Slusarski, D. C., Yang-Snyder, J., Busa, W. and Moon, R. T. (1997). Modulation of embryonic intracellular Ca^{2+} signaling by Wnt-5A. *Dev. Biol.* **182**, 114-120.

Snow, P. and Nuccitelli, R. (1993). Calcium buffer injections delay cleavage in Xenopus laevis blastomeres by dissipating Ca^{2+} gradients. *J. Cell Biol.* **122**, 387-394.

Speksnijder, J. E., Miller, A. L., Weisenseel, M. H., Chen, T. H. and Jaffe L. F. (1989). Calcium buffer injections block fucoid egg development by facilitating calcium diffusion. *Proc. Nat. Acad. Sci. USA* **86**, 6607-6611.

Stachel, S. E., Grunwald, D. J. and Myers, P. Z. (1993). Lithium perturbation and goosecoid expression identify a dorsal specification pathway in the pregastrula zebrafish. *Development* **117**, 1261-1274.

Stainier, D. Y. R., Lee, R. K. and Fishman, M. C. (1993). Cardiovascular development in the zebrafish. I. Myocardial fate map and heart tube formation. *Development* **119**, 31-40.

Webb, S. E., Lee, K. W., Karplus, E. and Miller, A. L. (1997). Localized calcium transients accompany furrow positioning, propagation, and deepening during the early cleavage period of zebrafish embryos. *Dev. Biol.* **192**, 78-92.

Wilding, M., Wright, E. M., Patel, R., Ellis-Davies, G. and Whitaker, M. (1996). Local perinuclear calcium signals associated with mitosis-entry in early sea urchin embryos. *J. Cell Biol.* **135**, 191-199.

Woo, K. and Fraser, S. E. (1995). Order and coherence in the fate map of the zebrafish nervous system. *Development* **121**, 2595-2609.

Yoon, C., Kawakami, K. and Hopkins, N. (1997). Zebrafish vasa homologue RNA is localized to the cleavage planes of 2- and 4-cell-stage embryos and is expressed in the primordial germ cells. *Development* **124**, 3157-3165.